

# Molecular Dynamics of Poly(*N*-isopropylacrylamide) in Protic and Aprotic Solvents Studied by Dielectric Relaxation Spectroscopy

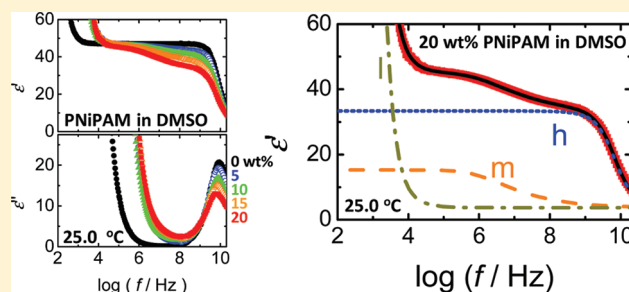
Shinya Nakano,<sup>†</sup> Yasuhiro Sato,<sup>†</sup> Rio Kita,<sup>\*,†</sup> Naoki Shinyashiki,<sup>†</sup> Shin Yagihara,<sup>†</sup> Seiichi Sudo,<sup>‡</sup> and Masaru Yoneyama<sup>§</sup>

<sup>†</sup>Department of Physics, Tokai University, Hiratsuka, Kanagawa 259-1292, Japan

<sup>‡</sup>Department of Physics, General Education Center, Tokyo City University, Tamazutsumi, Setagaya, Tokyo 158-8557, Japan

<sup>§</sup>Department of Chemistry and Chemical Biology, Gunma University, Kiryu, Gunma 376-8515, Japan

**ABSTRACT:** We report the experimental results of dielectric relaxation spectroscopy for the systems of poly(*N*-isopropylacrylamide) [PNiPAM] in various solvents in the frequency range of 40 kHz to 20 GHz at the solution temperature of 25.0 °C. The solvents used in this study were protic solvents (water, methanol, ethanol, and 1-propanol) and aprotic solvents (acetone, methyl ethyl ketone, and dimethyl sulfoxide). Two relaxation processes were observed at frequencies of approximately 1 MHz and 10 GHz in all the solutions. The origins of the two relaxation processes are considered to be the reorientation of dipoles of the PNiPAM chains at middle frequencies (m-process) and that of solvent molecules at higher frequencies (h-process). For the PNiPAM solutions composed of protic solvents except for 1-propanol, the relaxation time of the h-process increased with increasing PNiPAM concentration, whereas that of the h-process for the 1-propanol decreased with increasing PNiPAM concentration. In contrast, the relaxation times of the h-process for the aprotic solvents were independent of the density of hydrogen-bonding sites. For the m-process, the extrapolated relaxation time to zero polymer concentration  $\tau_{m0}$  was scaled by the solvent viscosity for all the protic solvents, whereas for the aprotic solvents  $\tau_{m0}$  showed no correlation with the solvent viscosity. The dynamics of polymer chains and solvent molecules in their solution state are clarified in terms of cooperative motion, which is associated with the interactions through hydrogen bonding at the molecular level.



## INTRODUCTION

Dielectric relaxation spectroscopy has been utilized for studying the molecular dynamics of polymer solutions.<sup>1–6</sup> In the case of polymer solutions composed of polar solvents in a solvent-rich region, relaxation processes due to the reorientation of dipoles of solvents and polymer chains are observed separately at higher and lower frequencies, respectively.<sup>3–5,7,8</sup> Typically, the relaxation process observed at frequencies on the order of 10 GHz is associated with the molecular motion of solvent molecules, while the relaxation process observed at kHz–MHz frequencies is attributed to the relaxation modes of polymer chains. The relaxation process owing to solvent molecules is affected by the addition of polymers.<sup>3,4,9–11</sup> This implies that the dynamical structures of solvent molecules are related to the polymers through interactions at the molecular level. The relaxation process that arises from the polymer chains should also be affected by the solvent molecules. This interdependence of polymer chains and solvent molecules can be analyzed by investigating the dielectric relaxation spectrum as a function of concentration and/or temperature. Dielectric relaxation spectra can be described by, for example, the relaxation time, the relaxation strength, and the shape parameter characterizing the distribution of the relaxation process. Therefore, the relaxation

parameters obtained by the variation of polymer concentration or temperature, as well as the solvent species, can provide important information leading to greater understanding of molecular interactions. Recently, the relaxation processes of polymer chains and solvent molecules have been studied systematically for the poly(vinylpyrrolidone) [PVP] system in various polar and nonpolar solvents in broad temperature and frequency ranges.<sup>3–5</sup> It has been revealed that the cooperation between segmental motion and the reorientation of solvent molecules provides intrinsic information about the molecular dynamics of polymer solutions.

In this study, we report the experimental results of dielectric relaxation behavior for the systems of poly(*N*-isopropylacrylamide) (PNiPAM) in protic and aprotic solvents as a function of PNiPAM concentration studied by dielectric relaxation spectroscopy. An aqueous solution of PNiPAM has a  $\Theta$ -temperature of 30.6 °C and undergoes a coil–globule transition upon heating.<sup>12–15</sup> The transition of PNiPAM chains in water is also observed upon the addition of a second water-miscible solvent, such as methanol,

**Received:** October 28, 2011

**Revised:** December 13, 2011

**Published:** December 15, 2011

tetrahydrofuran, or dioxane.<sup>16–19</sup> These thermally and solvent quality-sensitive responses of PNIPAM chains have attracted many researchers from the viewpoints of fundamental polymer physics and the possibility of practical application.<sup>20–23</sup> Indeed, there are many reports on PNIPAM solutions studied by, for example, scattering methods,<sup>12,13,17,24–26</sup> fluorescence,<sup>27</sup> IR spectroscopy,<sup>19,28,29</sup> calorimetry,<sup>30</sup> dielectric relaxation,<sup>6,7</sup> and theoretical methods.<sup>18,31,32</sup> PNIPAM chains can be dissolved in water, alcohols, and various organic solvents. Therefore, it is considered that PNIPAM solutions are suitable for studying molecular interactions by dielectric relaxation spectroscopy, which can be investigated over a wide range of magnitudes of the solvent dipole moment.

The solvents used in this study are divided into two types: protic and aprotic solvents. Water, methanol (MeOH), ethanol (EtOH), and 1-propanol (PrOH) were selected as the protic solvents, whereas the aprotic solvents used in this study are acetone (ACT), methyl ethyl ketone (MEK), and dimethyl sulfoxide (DMSO). The dynamics of PNIPAM in these solvents were measured by a broadband dielectric system in the frequency range of 40 kHz to 20 GHz at the solution temperature of 25.0 °C. This study reveals fundamental properties of the dynamics among polymer chains and solvent molecules, and the roles of molecular interactions via hydrogen bonding in PNIPAM solutions is clarified in detail.

## EXPERIMENTAL SECTION

Distilled and deionized water with an electrical conductivity of lower than 18.3  $\mu\text{S}/\text{m}$  was obtained using an ultrapure water product (Millipore, MILLI-Q Lab.). MeOH, EtOH, PrOH, ACT, MEK, and DMSO of analytical grade were purchased from Wako Pure Chemical Industry, and we used freshly opened bottles without further purification. The polymerization of PNIPAM is reported elsewhere.<sup>12</sup> The weight-averaged molecular weights  $M_w$  of PNIPAM used in this study were  $4.0 \times 10^2$  and  $4.1 \times 10^2$  kg/mol with molecular weight distributions  $M_w/M_n$  of 1.89 and 3.31, respectively, which were obtained using a GPC system.

Dielectric measurements were performed in the frequency range from 40 Hz to 20 GHz by time domain reflectometry (TDR) (Hewlett-Packard 54124T, 100 MHz to 20 GHz) and a precision impedance analyzer (Agilent Technologies 4294A, 40 to 110 MHz) at the temperature of the sample being 25.0 °C. A flat-end coaxial probe with a geometrical capacitance of  $1.35 \times 10^{-2}$  pF (electric length of 0.16 mm) was used for the dielectric measurements by TDR. Details of the apparatus and the procedures used in TDR were reported previously.<sup>33,34</sup> A coaxial cylindrical cell with a geometrical capacitance of 0.20 pF was used for the measurements with the impedance analyzer.

## RESULTS AND DISCUSSION

Figure 1 shows typical dielectric relaxation spectra obtained, where the real part  $\epsilon'$  and imaginary part  $\epsilon''$  of the complex permittivity are plotted as a function of frequency  $f$  for PNIPAM in DMSO. The dielectric relaxation process is observed in the vicinity of 10 GHz for pure DMSO, which is hereafter referred to as the h-process. The magnitude of the h-process decreases with the addition of PNIPAM. Additionally, a relaxation process appears in the vicinity of 1 MHz upon the addition of PNIPAM, which is observed in the real part and named the m-process. The magnitude of the m-process increases with increasing PNIPAM concentration. Therefore, the h- and m-process are attributed to

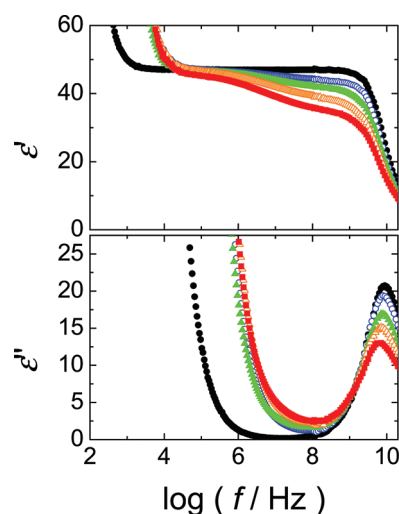


**Figure 1.** Real part  $\epsilon'$  and imaginary part  $\epsilon''$  of dielectric functions of 0 (●), 5 (blue ○), 10 (green ▲), 15 (orange △), and 20 wt % (red ■) PNIPAM in DMSO at 25.0 °C.

the reorientation of dipoles on the solvent molecules and the local chain motion of PNIPAM, respectively. The high-frequency portion of electrode polarization, named the l-process, is observed at approximately 10 kHz in the real part, and the contribution of dc conductivity is observed below 100 MHz in the imaginary part. Similar spectra were observed for the other PNIPAM solutions. To characterize these processes, a curve-fitting procedure was carried out. The dielectric constant and loss of PNIPAM solutions can be described as the summation of three relaxation processes and the contribution of dc conductivity as follows:

$$\begin{aligned} \epsilon^*(\omega) = & \epsilon_\infty + \frac{\Delta\epsilon_h}{1 + (j\omega\tau_h)^{\beta_h}} \\ & + \Delta\epsilon_m \int_0^\infty \left( -\frac{d\Phi_m}{dt} \right) \exp(-j\omega t) dt \\ & + \frac{\Delta\epsilon_l}{1 + (j\omega\tau_l)^{\beta_l}} - j\frac{\sigma}{\epsilon_0\omega}, \end{aligned} \quad (1)$$

$$\Phi_m = \exp \left\{ -\left( \frac{t}{\tau_{m,K}} \right)^{\beta_K} \right\},$$

where  $\omega$  is the angular frequency,  $t$  is the time,  $j$  is the imaginary unit given by  $j^2 = -1$ ,  $\epsilon_0$  is the dielectric constant in vacuum,  $\epsilon_\infty$  is the limiting high-frequency dielectric constant,  $\Delta\epsilon$  is the relaxation strength,  $\tau$  is the relaxation time,  $\beta$  is the symmetric broadening parameter ( $0 < \beta \leq 1$ ),  $\beta_K$  is the asymmetric broadening parameter ( $0 < \beta_K \leq 1$ ) of the Kohlrausch–Williams–Watts (KWW) function,<sup>35</sup> and  $\sigma$  is the conductivity. The subscripts h, m, and l denote the h-, m-, and l-processes, respectively. The subscript K indicates the KWW function. The h- and l-process are fitted well with the Cole–Cole equation<sup>36</sup> and the m-process can be described by the KWW equation<sup>35</sup> for all the PNIPAM solutions.

Figure 2 shows a typical example of the curve-fitting result obtained using eq 1, where the real part  $\epsilon'$  and imaginary part  $\epsilon''$  of complex permittivity are plotted as a function of the frequency

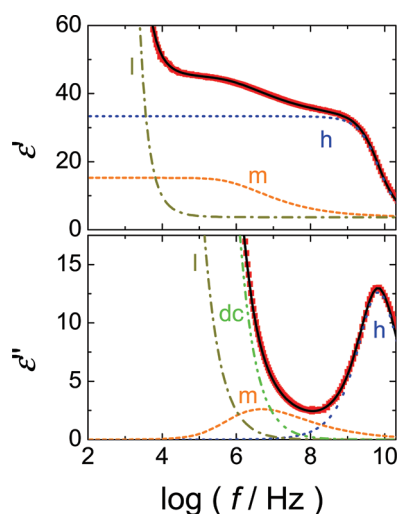


**Figure 2.** Real part  $\epsilon'$  and imaginary part  $\epsilon''$  of dielectric function of 20 wt % PNiPAM in DMSO at 25.0 °C. The lines were drawn using eq 1: dashed line, h-process; dotted line, m-process; dot-dash line, l-process; and double-dot-dash line, dc.

$f$  for PNiPAM in DMSO (20 wt %). The bold curve is the fitted curve, which shows good agreement with the data points. The obtained fitting results for the h-, m-, and l-processes and the contribution of dc conductivity are also shown. The relaxation time  $\tau_h$  of the h-process in the Cole–Cole equation agrees with the relaxation time obtained from the loss peak frequency. On the other hand, the relaxation time  $\tau_m$  of the m-process could not be simply determined using  $\tau_{m,K}$  in eq 1. Because the relaxation times in the empirical equation have no physical meaning and the method of estimating the relaxation time is still controversial. Therefore, we use the relaxation time  $\tau_m$  derived from the loss peak frequency of the m-process  $f_{mp}$  using the relation  $\tau_m = 1/(2\pi f_{mp})$ , because it is independent of the model and the most probable relaxation time. The dielectric loss peak of the l-process is outside the low-frequency limit of the measurement, and only its high-frequency tail is observed. Thus, the relaxation parameters of the l-process could not be correctly determined. To extract information on the m- and h-processes, we assumed that the dielectric loss peak frequency of the l-process was below our low-frequency limit, and an appropriate relaxation strength and shape parameter were obtained. The obtained dielectric relaxation parameters for all of the PNiPAM solutions are listed in Table 1.

Figure 3 shows the relaxation strengths of the h-process  $\Delta\epsilon_h$  and m-process  $\Delta\epsilon_m$  for all PNiPAM solutions as a function of PNiPAM concentration  $C$ . The h-process is observed in all pure solvents, and  $\Delta\epsilon_h$  decreases with increasing PNiPAM concentration. This behavior is mainly due to a decrease in the density of solvent molecules. On the other hand, the m-process is not observed in pure solvents, and  $\Delta\epsilon_m$  increases with increasing PNiPAM concentration. Therefore, the h- and m-processes are attributed to the reorientation of dipoles by the solvent molecules and the PNiPAM chains, respectively. The slope of  $\Delta\epsilon_m$  against the concentration  $C$  depends on the solvent species, even though the origin of the m-process is considered to be the local chain motion of PNiPAM. This result suggests that the relaxation strength of the m-process is correlated with the magnitude of the dipole moment of solvated solvents. It is also considered that there is cooperative motion among the local chains of PNiPAM,

the solvated molecules on PNiPAM, and the solvent molecules in the bulk. However, the origin of the relaxation strength of the m-process is not straightforward because the relaxation strength depends not only on the magnitude and the amount of the dipoles but also on the internal electric field and the directional correlation of dipoles. Nevertheless, the m-process is expected to be correlated with the local chain motion of polymer chains because the relaxation process occurs upon with the addition of the polymers. The origin and cooperative behavior of the m-process are further discussed below with respect to the relaxation times.

Figure 4 shows the relaxation times of the h-process  $\tau_h$  and the m-process  $\tau_m$  for all PNiPAM solutions as a function of PNiPAM concentration. The magnitude of  $\tau_m$  is at least several hundred times larger than that of  $\tau_h$ . The relaxation times  $\tau_h$  and  $\tau_m$  depend on the solvent species. To characterize the effect of the addition of PNiPAM on the relaxation process of the solvent molecules (h-process), the shift factor  $\tau_h/\tau_{h0}$  is plotted against the polymer concentration in Figure 5, where  $\tau_{h0}$  is the relaxation time of the pure solvent. The magnitude of  $\tau_h/\tau_{h0}$  increases with increasing PNiPAM concentration in all solutions except for the 1-propanol solution. In the 1-propanol solution,  $\tau_h/\tau_{h0}$  decreases with increasing PNiPAM concentration up to a concentration of 15 wt %. For polymer solutions, in general, the relaxation time of the solvent molecules increases with increasing polymer concentration, since the increase in the volume fraction of the polymer reduces the free volume available for the translational or rotational motion of solvent molecules. For protic solvents, the primary relaxation processes of alcohols and water are considered to be due to the cooperative dynamics of molecules accompanying the formation and deformation of intermolecular hydrogen bonding. The “wait-and-switch” (WS) model of the dielectric relaxation process for these solvents was proposed by Kaatz et al.<sup>37</sup> The WS model suggests that the relaxation time of protic solvent molecules is mainly determined by the behavior of the reorientation of the dipole moment on the hydroxyl group, which forms intermolecular hydrogen bonds and has to wait until favorable conditions for reorientation to occur. The rotational motion of the dipole moment is initiated by the presence of an additional neighboring hydroxyl group, which offers a site for the formation of a new hydrogen bond. Therefore, the main factor determining the relaxation time is the number density of hydrogen-bonding partners in the solution. The concentration of hydrogen-bonding partners  $C_{HB}$  of PNiPAM in protic solvents is defined by

$$C_{HB} = \rho \left( \frac{C_S N_S}{M_S} + \frac{C_P N_P}{M_P} \right) \quad (2)$$

Here,  $\rho$  is the density of the solution,  $C_S$  and  $C_P$  are the weight fractions of the solvent and PNiPAM,  $N_S$  and  $N_P$  are the numbers of hydrogen-bonding partners per solvent molecule and repeat unit of the polymer,  $M_S$  is the molecular weight of the solvent, and  $M_P$  is the molecular weight of a repeat unit of PNiPAM, respectively. For protic solvent systems,  $N_S$  and  $N_P$  are assumed to be 1 and 1.5, respectively. Although ACT, MEK, and DMSO do not belong to the series of protic solvents, we tentatively assumed that the three solvents have 1 hydrogen-bonding partners ( $N_S = 1$ ) to calculate the value of  $C_{HB}$ .

Figure 6 shows the relaxation time  $\tau_h$  of the h-process as a function of the concentration of hydrogen-bonding partners  $C_{HB}$

Table 1. Dielectric Relaxation Parameters Obtained for PNiPAM Solutions and the Viscosity of Solvents at 25.0 °C

solutions	C/wt %	$\varepsilon_\infty$	h-process			m-process			$\eta_s^a$ /mPa s
			$\Delta\varepsilon_h$	$\tau_h/s$	$\beta_h$	$\Delta\varepsilon_m$	$\tau_m/s$	$\beta_K$	
PNiPAM in water	0	5.2	72.7	$8.91 \times 10^{-12}{}^b$	1.00		$1.37 \times 10^{-8}{}^c$		0.890
	5.0	5.2	68.3	$1.02 \times 10^{-11}$	0.97	3.1	$1.55 \times 10^{-8}$	0.52	
	9.1	5.2	64.1	$1.08 \times 10^{-11}$	0.94	5.8	$1.74 \times 10^{-8}$	0.53	
	15.0	5.2	59.5	$1.26 \times 10^{-11}$	0.97	9.1	$1.95 \times 10^{-8}$	0.52	
	20.0	5.2	55.2	$1.35 \times 10^{-11}$	0.94	11.5	$2.27 \times 10^{-8}$	0.50	
PNiPAM in methanol	0	5.7	26.8	$5.01 \times 10^{-11}{}^b$	1.00		$1.00 \times 10^{-8}{}^c$		0.544
	4.9	5.2	26.3	$5.07 \times 10^{-11}$	0.98	1.4	$1.00 \times 10^{-8}$	0.54	
	10.7	4.2	25.7	$5.20 \times 10^{-11}$	0.97	2.6	$1.03 \times 10^{-8}$	0.57	
	15.0	4.7	22.4	$5.43 \times 10^{-11}$	0.98	4.8	$9.68 \times 10^{-9}$	0.51	
	20.0	4.1	21.8	$5.50 \times 10^{-11}$	0.98	5.6	$1.03 \times 10^{-8}$	0.53	
PNiPAM in ethanol	0	3.9	20.4	$1.51 \times 10^{-10}{}^b$	1.00		$2.74 \times 10^{-8}{}^c$		1.074
	4.9	3.7	19.7	$1.63 \times 10^{-10}$	1.00	1.0	$2.94 \times 10^{-8}$	0.54	
	10.3	3.8	18.5	$1.66 \times 10^{-10}$	0.99	2.1	$2.48 \times 10^{-8}$	0.53	
	15.0	3.6	17.8	$1.65 \times 10^{-10}$	0.97	2.9	$2.85 \times 10^{-8}$	0.56	
	20.3	3.2	16.5	$1.65 \times 10^{-10}$	0.97	4.4	$2.89 \times 10^{-8}$	0.50	
PNiPAM in 1-propanol	0	3.8	16.7	$3.15 \times 10^{-10}{}^b$	1.00		$4.64 \times 10^{-8}{}^c$		1.945
	5.0	3.6	15.4	$3.09 \times 10^{-10}$	1.00	1.0	$4.80 \times 10^{-8}$	0.47	
	9.5	3.7	14.5	$3.03 \times 10^{-10}$	1.00	1.8	$4.64 \times 10^{-8}$	0.50	
	14.7	3.3	13.9	$2.96 \times 10^{-10}$	0.97	2.6	$5.01 \times 10^{-8}$	0.50	
	17.8	3.2	13.5	$3.02 \times 10^{-10}$	0.96	2.8	$4.90 \times 10^{-8}$	0.52	
	20.0	3.5	12.6	$3.03 \times 10^{-10}$	0.94	3.5	$5.01 \times 10^{-8}$	0.47	
PNiPAM in acetone	0	1.9	18.9	$3.31 \times 10^{-12}{}^b$	1.00		$2.70 \times 10^{-8}{}^c$		0.306
	5.1	1.9	17.7	$3.63 \times 10^{-12}$	1.00	1.2	$2.86 \times 10^{-8}$	0.32	
	9.7	1.9	16.9	$3.63 \times 10^{-12}$	1.00	2.8	$3.00 \times 10^{-8}$	0.31	
	13.8	1.9	16.3	$3.89 \times 10^{-12}$	0.98	3.7	$3.07 \times 10^{-8}$	0.31	
	17.8	1.9	15.8	$4.17 \times 10^{-12}$	0.99	4.6	$3.28 \times 10^{-8}$	0.32	
PNiPAM in MEK	0	4.1	14.0	$5.25 \times 10^{-12}{}^b$	1.00		$2.72 \times 10^{-8}{}^c$		0.405
	5.0	4.1	13.2	$5.25 \times 10^{-12}$	0.98	1.3	$2.90 \times 10^{-8}$	0.34	
	10.0	4.1	12.4	$5.50 \times 10^{-12}$	0.94	2.8	$3.83 \times 10^{-8}$	0.34	
	15.0	4.1	11.6	$5.75 \times 10^{-12}$	0.94	4.0	$4.01 \times 10^{-8}$	0.34	
	20.5	4.1	10.7	$5.75 \times 10^{-12}$	0.94	5.0	$4.60 \times 10^{-8}$	0.34	
PNiPAM in DMSO	0	3.3	43.7	$2.04 \times 10^{-11}{}^b$	1.00		$1.64 \times 10^{-8}{}^c$		1.987
	5.1	2.2	41.3	$2.15 \times 10^{-11}$	0.99	3.2	$2.14 \times 10^{-8}$	0.42	
	10.0	3.0	37.7	$2.30 \times 10^{-11}$	0.96	5.7	$2.34 \times 10^{-8}$	0.41	
	15.0	3.0	34.1	$2.48 \times 10^{-11}$	0.94	9.0	$3.09 \times 10^{-8}$	0.40	
	20.1	3.2	30.0	$2.71 \times 10^{-11}$	0.92	11.6	$3.83 \times 10^{-8}$	0.41	

<sup>a</sup> The viscosity of pure solvents  $\eta_s$  is taken from ref 41. <sup>b</sup> The relaxation time of pure solvents which is designated as  $\tau_{h0}$  in the texts. <sup>c</sup> The relaxation time of m-process at 0 wt % of polymer concentration is the extrapolated value and designated as  $\tau_{m0}$  in the texts.

for all the PNiPAM solutions. The plots of  $\tau_h$  for pure water and the alcohols are given by closed circles that lie on a straight line, as predicted by the WS model. The relaxation times  $\tau_h$  for the solutions of alcohols and water except for 1-propanol increase monotonically with decreasing  $C_{HB}$  as shown by arrows. In contrast, for the 1-propanol solution the relaxation time  $\tau_h$  decreases with increasing  $C_{HB}$ . Note that not only the relaxation times of the pure alcohols and pure water but also those of the polymer solutions of various concentrations appear to lie on the straight line. The water solution has relatively large values of  $C_{HB}$  and undergoes the greatest change in  $\tau_h$ , whereas the alcohol solutions exhibit smaller changes in  $\tau_h$ . This behavior of  $\tau_h$  indicates that the total number of possible hydrogen bonds in the system dominates the relaxation time of solvent molecules in

the solution. Similar results have been observed in other systems; PVP in alcohols and in water show comparable behavior to PNiPAM solutions,<sup>4</sup> even though  $C_{HB}$  for PVP solution is different from that for PNiPAM solution owing to the difference in the chemical composition. The concentration of hydrogen-bonding partners per repeat unit of the polymer  $N_p$  for PVP systems was assumed to be 1.<sup>4</sup> On the other hand, in this study on PNiPAM solutions,  $N_p$  for PNiPAM is assumed to be 1.5. Ono and Shikata studied the dielectric relaxation of PNiPAM in water by a dielectric relaxation method, and reported that the repeat unit of PNiPAM undergoes the solvation with about 11 water molecules below 30 °C.<sup>7</sup> However, it is stressed that, the value  $N_p = 1.5$  for PNiPAM estimated in this work is the concentration of hydrogen-bonding partners per repeat unit of the polymer, not



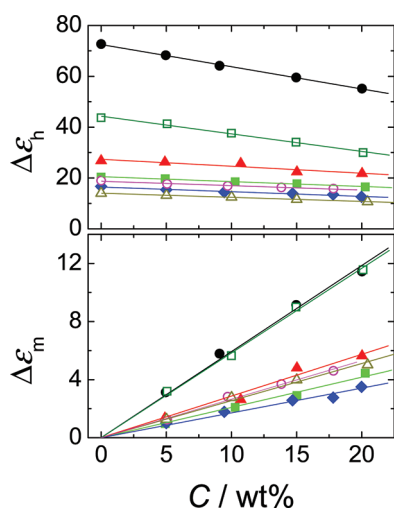


**Figure 3.** Relaxation strengths of the h-process  $\Delta\epsilon_h$  and m-process  $\Delta\epsilon_m$  against polymer concentration for PNIPAM solutions with water (●), methanol (red ▲), ethanol (green ■), 1-propanol (blue ◆), acetone (red ○), MEK (olive △), and DMSO (green □) at 25.0 °C.

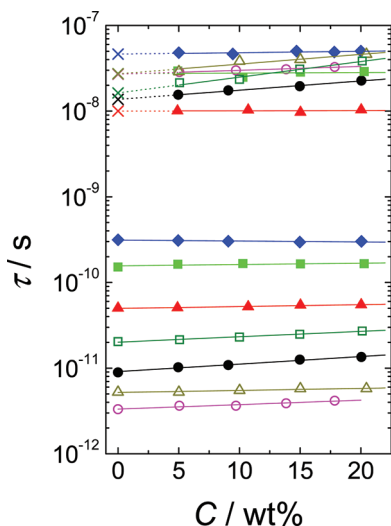


**Figure 4.** Relaxation times of the h-process  $\tau_h$  and m-process  $\tau_m$  against polymer concentration for PNIPAM solutions with water (●), methanol (red ▲), ethanol (green ■), 1-propanol (blue ◆), acetone (red ○), MEK (olive △), and DMSO (green □) at 25.0 °C. The crosses are extrapolated values of the relaxation time of the m-process for the pure solvents.

the number of solvated water molecules. In Figure 6 the values of  $\tau_h$  for ACT, MEK, and DMSO solutions are also plotted; these values show no correlation with  $\tau_h$  for PNIPAM solutions composed of the protic solvents. The observed relaxation process of the protic solvents of water and alcohols is considered to be due to the cooperative dynamics of molecules accompanying the formation and deformation of molecular interactions through intermolecular hydrogen bonding. On the other hand, the relaxation process of the aprotic solvents ACT, MEK, and DMSO is considered to involve the common molecular dynamics of rotational diffusion related to the viscosity without interactions via hydrogen bonding.

For all the solvents the relaxation time  $\tau_m$  of the m-process increases with increasing PNIPAM concentration (Figure 4). In

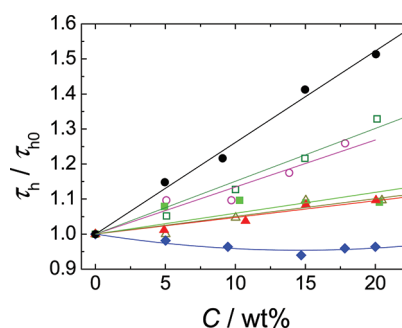


**Figure 5.** Shift factor of relaxation time of the h-process against polymer concentration for PNIPAM solutions with water (●), methanol (red ▲), ethanol (green ■), 1-propanol (blue ◆), acetone (red ○), MEK (olive △), and DMSO (green □) at 25.0 °C. The relaxation times of the h-process were normalized by the relaxation time of each solvent to obtain the shift factor  $\tau_h/\tau_{h0}$  of the relaxation time.

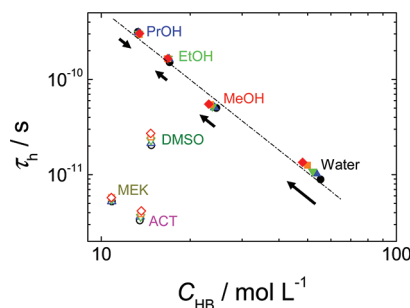


**Figure 6.** Plots of relaxation time  $\tau_h$  of the h-process against concentration of hydrogen-bonding partners  $C_{HB}$  for PNIPAM solutions with polymer concentrations of 0 (●), 5 (blue ▲), 10 (green ▼), 15 (orange ■), and 20 wt % (red ◆) at 25.0 °C. The closed symbols and open symbols show the solutions with protic solvents and aprotic solvents, respectively. The arrows mean the increasing direction of PNIPAM concentration and the accurate concentrations of polymers are found in TABLE 1.

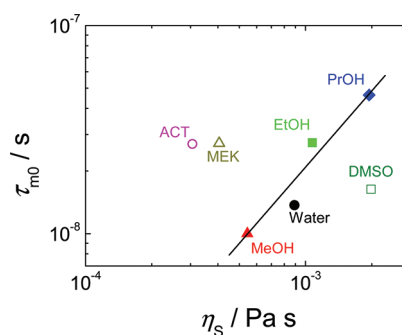


**Figure 7.** Plots of relaxation time of the m-process extrapolated to zero PNIPAM concentration  $\tau_{m0}$  against solvent viscosity  $\eta_s$  at 25.0 °C. The solvents of the PNIPAM solutions are water (●), methanol (red ▲), ethanol (green ■), 1-propanol (blue ◆), acetone (red ○), MEK (olive △), and DMSO (green □).

pure solvents, the m-process does not occur, but we show the values of the relaxation time extrapolated to 0 wt %, denoted as crosses in Figure 4, which are designated as  $\tau_{m0}$ . The value of  $\tau_{m0}$  indicates the relaxation time of an isolated PNIPAM chain at infinite dilution of PNIPAM. Figure 7 shows plots of  $\tau_{m0}$  against

the viscosity  $\eta_s$  of the pure solvents. At first glance, the plots in Figure 7 appear to be scattered. The relationship between  $\tau_{m0}$  and  $\eta_s$  has been studied experimentally for various systems and the following expression holds:

$$\tau_{m0} \propto \eta_s^n \quad (3)$$

Values of  $n$  in the range of 0.74–1.3 have been obtained for various systems.<sup>3,4,38,39</sup> In this study of PNiPAM solutions, for all the protic solvents, i.e., water, MeOH, EtOH, and PrOH,  $\tau_{m0}$  exhibits a linear relation against  $\eta_s$  and the exponent  $n$  in eq 3 was obtained as  $1.2 \pm 0.2$  by least-squares fitting. Here,  $\pm$  denotes one standard deviation. The fitted result is shown as a solid line in Figure 7. On the other hand, a simple correlation between  $\tau_{m0}$  against  $\eta_s$  such as that described by eq 3 was not observed for the PNiPAM solutions composed of the aprotic solvents ACT, MEK, and DMSO. The behavior of  $\tau_{m0}$  for PNiPAM can clearly be classified into two types depending on the type of solvent, i.e. protic or aprotic. Whether or not the relaxation times obtained for the m-process lie on the straight line given by eq 3 is considered to arise from the ability of the solvent molecules to form hydrogen bonds. According to the Debye–Stokes equation,<sup>40</sup> the relationship between the relaxation time and solvent viscosity is given by

$$\tau_0 = \frac{V}{k_B T} \eta_s \quad (4)$$

where  $k_B$  is Boltzmann's constant,  $V$  is the effective volume of a moving unit, and  $T$  is the absolute temperature. For solutions of PVP in alcohols and in chloroform, the plots of  $\tau_{m0}$  vs  $\eta_s$  lie on a single straight line, regardless of the polarity and hydrogen-bonding ability of the solvent.<sup>4,5</sup> In contrast, the results for PNiPAM solutions composed of aprotic solvents suggest that the local chain motion of PNiPAM is affected by not only the solvent viscosity but also the other molecular interactions, e.g., the effect of hydrogen-bonding ability or the cooperative nature depending on the systems. These results are speculated to be related to the structure of the polymer; vinylpyrrolidone (VP), the repeat unit of PVP, only has an acceptor site, whereas *N*-isopropylacrylamide (NiPAM) the repeat unit of PNiPAM, has both a donor site and an acceptor site, providing it with hydrogen-bonding ability. Furthermore, NiPAM has a hydrophobic region, where interactions may occur through hydrophobic hydration in water.<sup>20</sup> These facts indicate that hydrogen bonding has a significant role in the relaxation process of solvent molecules as well as the local chain motion of PNiPAM. This may be related to the more complex behavior of the dynamics of PNiPAM systems compared with those in PVP systems.

## CONCLUSION

Two dielectric relaxation processes due to the reorientation of dipoles on the local chain of PNiPAM and solvent molecules were observed in several solutions composed of protic solvents (water, MeOH, EtOH, and PrOH) and aprotic solvents (ACT, MEK, and DMSO) by broadband dielectric spectroscopy at 25.0 °C. The interdependence between the PNiPAM chains and solvent molecules was clarified as follows. The relaxation time  $\tau_h$ , which originates from the reorientational motion of protic solvents in the PNiPAM solution, is scaled by the concentration of hydrogen-bonding partners. On the other hand, for the aprotic solvents ACT, MEK, and DMSO,  $\tau_h$  shows no correlation with the scaled relation found for the protic solvents.

The results indicate that the relaxation process of solvent molecules is dominated by the density of hydrogen-bonding sites in the PNiPAM solution. The relaxation time of the m-process at infinite dilution  $\tau_{m0}$ , which is the relaxation time extrapolated to a zero concentration of PNiPAM, is scaled by the solvent viscosity of the protic solvents, while  $\tau_{m0}$  for PNiPAM in aprotic solvents shows no correlation with the solvent viscosity. The solvent-dependent behavior of the relaxation process of the local chain motion of PNiPAM (m-process) suggests that the dynamics of PNiPAM chains depends on the type of solvent, which is classified into the two categories of protic and aprotic solvents. The results mean that the molecular interactions that occur through hydrogen bonding, i.e., the interdependence of PNiPAM chains and solvent molecules via hydrogen bonding have a dominant role in the molecular motion of PNiPAM chains. This dielectric relaxation study on PNiPAM solutions composed of various solvents has provided an insight into the role of hydrogen-bonding ability in the system as well as that of solvent viscosity.

## AUTHOR INFORMATION

### Corresponding Author

\*E-mail: rkita@keyaki.cc.u-tokai.ac.jp.

## ACKNOWLEDGMENT

This work was partially supported by a Grant-in-Aid for Scientific Research from MEXT, Japan, and a Research and Study Project of the General Research Organization of the Tokai University Educational System.

## REFERENCES

- (1) Nakazawa, M.; Urakawa, O.; Adachi, K. *Macromolecules* **2000**, *33*, 7898.
- (2) Yada, M.; Nakazawa, M.; Urakawa, O.; Morishima, Y.; Adachi, K. *Macromolecules* **2000**, *33*, 3368.
- (3) Shinyashiki, N.; Sengwa, R. J.; Tsubotani, S.; Nakamura, H.; Sudo, S.; Yagihara, S. *J. Phys. Chem. A* **2006**, *110*, 4953.
- (4) Shinyashiki, N.; Imoto, D.; Yagihara, S. *J. Phys. Chem. B* **2007**, *111*, 2181.
- (5) Shinyashiki, N.; Spanoudaki, A.; Yamamoto, W.; Nambu, E.; Yoneda, K.; Kyritsis, A.; Pissis, P.; Kita, R.; Yagihara, S. *Macromolecules* **2011**, *44*, 2140.
- (6) Ono, Y.; Shikata, T. *J. Phys. Chem. B* **2007**, *111*, 1511.
- (7) Ono, Y.; Shikata, T. *J. Am. Chem. Soc.* **2006**, *128*, 10030.
- (8) Spanoudaki, A.; Shinyashiki, N.; Kyritsis, A.; Pissis, P. *AIP Conf. Proc.* **2008**, *982*, 125.
- (9) Murthy, S. S. N. *J. Phys. Chem. B* **2000**, *104*, 6955.
- (10) Tyagi, M.; Murthy, S. S. N. *Carbohydr. Res.* **2006**, *341*, 650.
- (11) Shinyashiki, N.; Matsumura, Y.; Mashimo, S.; Yagihara, S. *J. Chem. Phys.* **1996**, *104*, 6877.
- (12) Kubota, K.; Fujishige, S.; Ando, I. *J. Phys. Chem.* **1990**, *94*, 5154.
- (13) Kubota, K.; Fujishige, S.; Ando, I. *Polym. J.* **1990**, *22*, 15.
- (14) Wang, X.; Qiu, X.; Wu, C. *Macromolecules* **1998**, *31*, 2972.
- (15) Wang, X.; Wu, C. *Macromolecules* **1999**, *32*, 4299.
- (16) Winnik, F. M.; Ringsdorf, H.; Venzmer, J. *Macromolecules* **1990**, *23*, 2415.
- (17) Zhang, G.; Wu, C. *J. Am. Chem. Soc.* **2001**, *123*, 1376.
- (18) Tanaka, F.; Koga, T.; Winnik, F. M. *Phys. Rev. Lett.* **2008**, *101*, 028302.
- (19) Katsumoto, Y.; Tanaka, T.; Ihara, K.; Koyama, M.; Ozaki, Y. *J. Phys. Chem. B* **2007**, *111*, 12730.
- (20) Schild, H. G. *Prog. Polym. Sci.* **1992**, *17*, 163.

- (21) Kita, R.; Wiegand, S. *Macromolecules* **2005**, *38*, 4554.
- (22) Kita, R.; Polyakov, P.; Wiegand, S. *Macromolecules* **2007**, *40*, 1638.
- (23) Katsumoto, Y.; Kubosaki, N. *Macromolecules* **2008**, *41*, 5955.
- (24) Wu, C.; Zhou, S. *Macromolecules* **1995**, *28*, 5388.
- (25) Kawaguchi, T.; Kobayashi, K.; Osa, M.; Yoshizaki, T. *J. Phys. Chem. B* **2009**, *113*, 5440.
- (26) Nakano, S.; Ogiso, T.; Kita, R.; Shinyashiki, N.; Yagihara, S.; Yoneyama, M.; Katsumoto, Y. *J. Chem. Phys.* **2011**, *135*, 114903.
- (27) Winnik, F. M. *Macromolecules* **1990**, *23*, 233.
- (28) Katsumoto, Y.; Tanaka, T.; Sato, H.; Ozaki, Y. *J. Phys. Chem. A* **2002**, *106*, 3429.
- (29) Maeda, Y.; Higuchi, T.; Ikeda, I. *Langmuir* **2000**, *16*, 7503.
- (30) Kujawa, P.; Winnik, F. M. *Macromolecules* **2001**, *34*, 4130.
- (31) Okada, Y.; Tanaka, F. *Macromolecules* **2005**, *38*, 4465.
- (32) Tanaka, F.; Koga, T.; Kojima, H.; Winnik, F. M. *Macromolecules* **2009**, *42*, 1321.
- (33) Capaccioli, S.; Ngai, K. L.; Ancherbak, S.; Rolla, P. A.; Shinyashiki, N. *J. Non-Cryst. Solids* **2011**, *357*, 641.
- (34) Sudo, S.; Shinyashiki, N.; Kitsuki, Y.; Yagihara, S. *J. Phys. Chem. A* **2002**, *106*, 458.
- (35) Williams, G.; Watts, D. C. *Trans. Faraday Soc.* **1970**, *66*, 80.
- (36) Cole, K. S.; Cole, R. H. *J. Chem. Phys.* **1941**, *9*, 341.
- (37) Kaatz, U.; Behrends, R.; Pottel, R. *J. Non-Cryst. Solids* **2002**, *305*, 19.
- (38) Mashimo, S. *Macromolecules* **1976**, *9*, 91.
- (39) Adolf, D. B.; Ediger, M. D.; Kitano, T.; Ito, K. *Macromolecules* **1992**, *25*, 867.
- (40) Debye, P. *Polar Molecules*; Dover Publications: New York, 1929.
- (41) *CRC Handbook of Chemistry and Physics*; 92nd ed.; Haynes, W. M., Ed.; CRC Press: Boca Raton, FL, 2011.